UNIVERSITY OF CALIFORNIA SAN DIEGO

Investigating the role of ZFP36L2 on the stability of mRNAs encoding histone lysine demethylases in cancer

A Thesis submitted in partial satisfaction of the requirements

for the degree Master of Science

in

Biology

by

Sina Ghaffarnejad

Committee in Charge:

Professor Heidi Cook-Andersen, Chair
Professor Jens Lykke-Andersen
Professor Miles Wilkinson

2022

The thesis of Sina Ghaffarnejad is approved, and it is acceptable in quality and form for publication on microfilm and electronically.

University of California San Diego

2022

Table of Contents

List of Abbreviations

ARE	Adenine-Uridine Rich Elements
HDAC	Histone Lysine Deacetylase
HMT	Histone Methyltransferase
KDM	Histone Lysine Demethylase
ZFP36L2	ZFP36 ring finger protein like 2
UTR	Untranslated Region
MNP	Myeloproliferative Neoplasms
AML	Acute Myeloid Leukemia
H3K4me3	Histone 3 Lysine 4 trimethyl
H3K9me3	Histone 3 lysine 9 trimethyl
RNA-seq	RNA sequencing
EISA	Exon-Intron Split Analysis
ORF	Open Reading Frame
FDR	False Discovery Rate

List of Figures

List of Tables

Acknowledgements

I would like to thank Dr. Heidi Cook-Andersen, my Principal Investigator, Mentor, and Chair for all the support and encouragement, she provides me to become a critical and effective scientist. The Cook-Andersen lab facilitated a rapid learning environment to learn many new groundbreaking techniques as well as taught me how to think and analyze like a scientist. It encouraged me to push my boundaries and attempt to develop methods and ideas independently while offering assistance and guidance when needed.

I would also like to thank Dr. Jens Lykke-Andersen and Dr. Miles Wilkinson for joining my committee even in these difficult times due to the COVID-19 pandemic.

I would also like to acknowledge Dr. Kyucheol Cho and Olcay Soyalan, for initiating me into the laboratory and helping me develop the foundational skills needed for my success. Additionally, I'd like to thank Dr. Joseph Owen for his guidance in helping me design a technique to knockout ZFP36L2 using CRISPR-Cas9.

To all the current members of the Cook-Andersen Lab, I want to thank you for contributing to such a welcoming and collaborative environment. Being in a comfortable environment that I with people that are inviting and supportive was memorable and critical for my success. I hope to maintain this form of chemistry with my colleagues in all my experiences moving forward and support younger students that are in a similar situation as I was when first joining the lab. To all the current members of the Cook-Andersen Lab, I want to thank you for contributing to such a welcoming and collaborative environment. Being in a comfortable environment that I with people that are inviting and supportive was memorable and critical for my success. I hope to maintain this form of chemistry with my

colleagues in all my experiences moving forward and support younger students that are in the similar situation I was when first joining the lab.

Abstract of the Dissertation

Investigating the role of ZFP36L2 on the stability of mRNAs encoding histone lysine demethylases in cancer

By

Sina Ghaffarnejad

Master of Science in Biology

University of California San Diego, 2022

Professor Heidi Cook-Andersen, Chair

Epigenetic regulation is at the forefront of cancer research. Histone lysine demethylases (KDMs) is a class of histone modifying factors that show considerable promise for treating various cancer types, including leukemia, colon cancer, and breast cancer. ZFP36L2, an mRNA decay activator, has previously been shown to regulate

multiple KDMs, including *KDM4B*, *KDM4C*, and *KDM5B*. Mutations in the *ZFP36L2* gene have been associated with many cancer types, including acute myeloid leukemia (AML) and colorectal cancer. My study aims to investigate the relationship between ZFP36L2 and histone lysine demethylases in malignant cells through both experimental and computational analysis. Towards these goals, I generated HeLa cells with stably repressed *ZFP36L2* expression using the CRISPR-Cas9 technique. These *ZFP36L2*-knockdown cells were used to assess changes in the expression levels of KDMs and changes in cell proliferation. My experiments suggested that these *ZFP36L2*-knockdown cells had decreased cell proliferation, implying ZFP36L2 is a negative regulator of cell proliferation and is not due to ZFP36L2's previously reported ability to destabilize ARE-containing histone lysine demethylases mRNAs, as my *ZFP36L2*-knockdown cells had expression of KDM mRNAs. To assess the effect of *ZFP36L2* loss in a different type of cancer, I analyzed a published RNA-seq dataset of *ZFP36L2*-knockout AML cells using a published algorithm to infer mRNA stability. I asked if the loss of *ZFP36L2* results in an increase of stability in KDM transcripts. I identified a small subset of mRNAs that are either significantly stabilized or destabilized. However, no KDM mRNAs regulated by ZFP36L2 were identified.

Introduction

Currently, one of the most dynamic fields of research is epigenomics. Epigenomic research is the study of gene regulation associated with systematic changes that exclude permanent alterations to the genome. One major focus of epigenomics are histone modification and the interaction between DNA and histones (Elvir, 2019). Genomic DNA is naturally condensed into chromatin structures, which are formed through the interaction of DNA with charged histone proteins such as histone H3 and H (Hsiang, 1977). The condensation of genomic DNA serves two reasons 1.) to condense the genome in order to fit into the nucleus (Sakamoto, 2004) and 2.) to regulate gene expression through regulating the accessibility of gene promoters and other regulatory regions to nonhistone proteins (Kouzarides, 2007).

Because these histone modifications are associated with gene regulation, they have emerged as a major focus in cancer therapy (Mohammad, 2019). Currently, there are multiple drug candidates being developed to inhibit histone modifiers to suppress cancer growth (Khan, 2019) (Said, 2001). These candidates focus on targeting histone deacetyl transferases (HDACs) (Suraweera, 2018) and histone methyl transferases (HMTs) (Kim, 2003) that either add or remove acetyl and methyl groups from histone residues, respectively. These therapies have been shown to inhibit the growth of certain cancers such as breast (Bian, 2018) and colorectal cancer (Wang, 2021). Although HDACs and HMTs inhibitors are the primary therapeutics currently being developed as therapies to target oncogenic histone modifying factors, many other classes of histone modifiers are also being researched for their therapeutic potential.

Histone lysine demethylases (KDMs) are another major class of histone modifying proteins that remove methyl groups from lysine residues within histone proteins (Klose, 2006). Demethylation has been shown to promote gene expression in certain cases (Ishimura, 2009) while repressing gene expression in other cases (Cai, 2011). Clinical data shows that different cancers, including hepatocellular carcinoma (Kim, 2019), prostate cancer (Kahl, 2006), as well as colorectal cancer (Kogure, 2013), are correlated with KDM deregulation and that certain KDMs, such as *KDM1A*, are highly upregulated in patients with a worse prognosis (Hou, 2021). This suggests that KDMs may be a critical target for cancer progression and that therapeutics targeting KDMs may have potential in mitigating tumor growth and possibly promoting its regression.

Aside from histone modifiers, another target for cancer therapeutics are regulatory factors that control the expression of many genes simultaneously. *ZFP36L2*, and its paralogs tristetraprolin and *ZFP36L1*, are RNA-binding proteins (RBPs) that regulate decay of a broad range of protein-coding transcripts (Mukherjee, 2014). ZFP36L2 is a zinc-finger protein that binds mRNAs and promotes their decay through the recruitment of mRNA degradation complexes (Lykke-Andersen, 2005). ZFP36L2 has been described to bind mRNAs that have adenine-uridine rich elements (AREs) in their 3' UTRs and recruits mRNA decay enzymes that lead to the decapping and deadenylation of all mRNA targets containing a 3' UTR ARE (Brooks and Blackshear, 2013).

Like KDMs, *ZFP36L2* has also been shown to be dysregulated in various cancers. Clinical data from patients with Philadelphia-negative chronic myoproliferative neoplasms (MPNs) showed that *ZFP36L2* was significantly downregulated in tumor cells (Skov,

2019). In a genomic screen of colorectal carcinoma samples, *ZFP36L2* was also found to be among the most significantly deregulated genes (Bertucci, 2004).

Furthermore, examinations of ZFP36L2 have found a connection between *ZFP36L2* expression and a few critical hallmarks of cancer. In an acute myeloid leukemia (AML) cell line model, Liu et al showed that the overexpression of *ZFP36L2* leads to lower rates of cell proliferation and higher rates of cell differentiation, cell-cycle arrest, and apoptosis (Liu, 2018). Similar findings have also been reported in colorectal cancer models (Suk, 2018). In addition to these findings, ZFP36L2 has also been reported to play an oncogenic role in cancer. Yonemori et al reported that ZFP36L2 promote cell aggression and surrounding tissue damage in pancreatic ductal adenocarcinoma (Yonemori, 2017). Furthermore, it was reported that the silencing of *ZFP36L2* in glioblastoma cell models increases the cells' sensitivity to the chemotherapy temozolomide and induces G2/M cell cycle arrest and apoptosis (Che Mat, 2021). Given this inconsistency in the literature, there is a need to further investigate the role of ZFP36L2 in cancer and determine its mechanism to help explain why there is so much variability when examining it in different cancer models.

Our team has previously published data indicating that ZFP36L2 plays a major role in the regulation of KDM expression. Levels of multiple KDMs were found to increase as a group with knockout of *ZFP36L2* in mouse oocytes (Dumdie, 2018). To ask if ZFP36L2 regulates the mRNAs at the level of mRNA stability, Dumdie et al transiently knocked out ZFP36L2 in HeLa cells, then treated the cells with Actinomycin D, which is a common inhibitor of transcription (Perry, 1970). qRT-PCR was carried out on extracted RNA from the treated and untreated cells, which revealed a significant increase in the half-life of

mRNA for various lysine demethylases. These KDMs include *KDM1B, KDM3C, KDM4B, KDM4C, KDM5B, and KDM5C,* each of which were found to contain an ARE in their 3'UTR. These studies demonstrated that ZFP36L2 targeted the transcripts of multiple different KDMs for degradation in human HeLa cells via a mechanism likely conserved in mouse oocytes.

It is important to note that most of the KDMs found to be decay targets of ZFP36L2 act on lysine residues of either H3K4me3 or H3K9me3 to remove methyl groups. H3K4me3 is well established as a histone modification that activates transcription through the formation of euchromatin (Howe, 2016). On the other hand, H3K9me3, is associated with gene repression, due to the formation of heterochromatin (Nicetto, 2019). Of the KDM mRNAs destabilizes by ZFP36L2, several encode proteins that demethylate H3K4me3 – including *KDM1B*, *KDM5B*, and *KDM5C* (Ciccone, 2009, Xhabija, 2019, Outchkourov, 2013). These factors contribute to multiple processes, including embryonic cell differentiation and oncogenic control (Dey, 2008, He, 2022). On the other hand, other KDM mRNAs targeted by ZFP36L2—namely *KDM3C, KDM4, and KDM4C*—are known to demethylate the repressive mark H3K9me3 (Lee, 2019, Duan, 2019, Yuan, 2016). Of potential significance to cancer, H3K9me3 has been a major target for AML therapeutic development due to the major clinical findings that show AML patients' DNAs are hypomethylated, specifically on H3K9 (Monaghan, 2019).

Given previous findings from Dumdie et al, it is hypothesized that ZFP36L2 is mechanistically connected to KDM expression by being a directly inducing decay of their mRNA transcripts. Furthermore, it is hypothesized that KDMs are highly deregulated in cancers, in addition to ZFP36L2. Furthermore, it has been shown that ZFP36L2 has

several tumor suppressive effects on multiple cell types, however, the mechanism of how ZFP36L2 carries out its tumor suppressive actions has still yet to be determined.

In this study, we generated a *ZFP36L2* heterozygous knockout model to investigate the relationship between ZFP36L2 and KDMs to determine if ZFP36L2 is a direct or indirect regulator of KDM expression.

Hypothesis

Given previous findings from Dumdie et al, it is hypothesized that:

- ZFP36L2 is mechanistically connected to KDM expression by directly inducing decay of their mRNA transcripts.
- Dysregulation of KDMs by ZFP36L2 contributes to the proliferation and/or survival of cancer cells
- These roles are mechanistically linked—i.e., that regulation of KDM expression by ZFP36L2 is important for cell proliferation and/or survival.

It has been shown that ZFP36L2 has several tumor suppressive effects on multiple cell types; however, the mechanism of how ZFP36L2 carries out its tumor suppressive actions has still yet to be determined. That regulation of KDM levels by ZFP36L2 might play an important role is an interesting possibility.

Specific Aims

Given the inconsistencies in published data regarding ZFP36L2 and its role in cancer development, this project was designed to further understand the relationship between ZFP36L2 and its association with histone modifications factors such as histone lysine demethylases. This project will be divided between three specific Aims.

Aim 1: Does the stable repression of *Zfp36L2* stably upregulate KDM expression? This first focus will be to investigate the findings of Dumdie et al further to determine if the stable downregulation of *ZFP36L2* yields comparable KDM transcript levels as to when it was transiently downregulated. An experimental approach will be used to design a method to knockout genomic expression of *ZFP36L2* in HeLa cells and assess the effects on the deregulation of histone modification factors.

Aim 2: Does ZFP36L2 regulate cell proliferation in HeLa cells? The second focus of this thesis will be to determine if the changes induced by the stable downregulation of *ZFP36L2* causes alterations in cell proliferative rate. This aim is intended to draw a connection between the findings of Dumdie et al and cancer to determine if ZFP36L2's role in cancer is connected to the deregulation of KDMs.

Aim 3: Does ZFP36L2 act to degrade KDM mRNAs in an AML cancer model? The final focus of this thesis will be to independently analyze RNA-seq data from a previously published study done by (Wang, 2021) in a different cancer cell line. The RNA-seq data from this study is from the acute myeloid leukemia cell model, MOLM-13, which has had ***ZFP36L2*** knocked out using a CRISPR-Cas9 system. This will allow us to begin to ask how reproducible our findings in Hela cells are in other cancer cell lines.

Together, these studies are important steps toward understanding whether ZFP36L2 plays a significant role in regulation of KDM mRNA levels and in cell proliferation in cancer cells--and whether these potential roles for ZFP36L2 are mechanistically linked.

Results

Plan to knockout Zfp36l2 in Hela cells by CRISPR

In recent years, CRISPR-Cas9 has quickly developed to being a relatively quick and accurate method to inducing deletions in the genome of cells (Wang, 2016). To stably assess the changes in KDM regulation, a CRISPR-based method to knockout *ZFP36L2* coding sequence was implemented, using two independent gRNAs targeting both the upstream and downstream genomic regions of *ZFP36L2*. Since *ZFP36L2* has a rather small genomic sequence, the expectation was that the simultaneous double-stranded breaking of *ZFP36L2* in the promoter region and in the second exon will induce a non-homologous end joining event that will remove the *ZFP36L2* coding sequence entirely while rejoining the DNA strands by combining the cut sites of both gRNAs. A schematic of this process can be found in **Figure 1**.

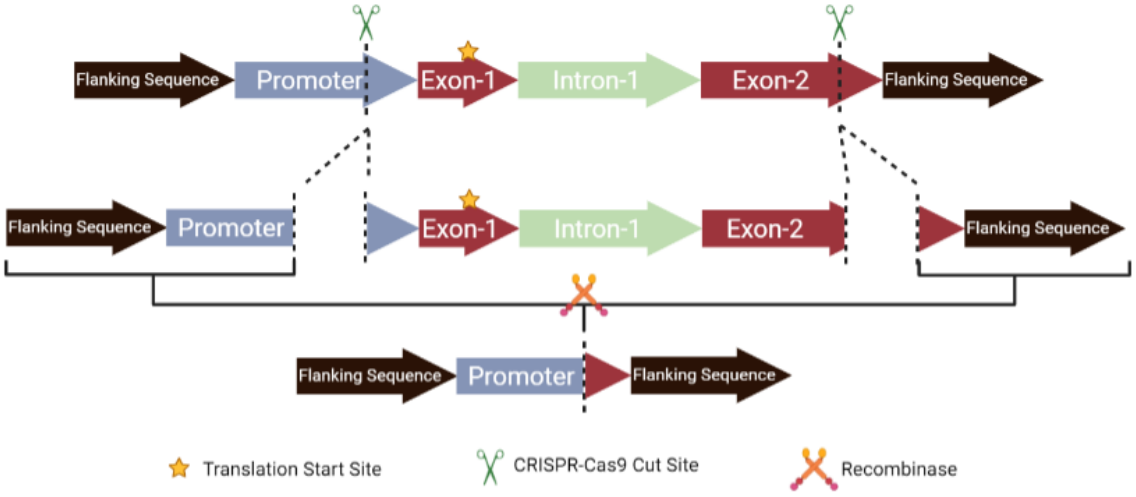

Figure 1: Schematic of method to knockout ZFP36L2

Design of guide RNAs (gRNAs)

To develop a HeLa stable variant with *ZFP36L2* knocked out, gRNAs were designed and aligned against the human genome to determine top gRNA candidates for Streptococcus pyogenes Cas9 (SpCas9). These candidates were designed to have perfect alignment to the genomic sequence of *ZFP36L2*, while minimizing non-specificity and off-target digestion. Wild-type HeLa genomic DNA was sequenced using Sanger Sequencing to determine the exact genomic sequence for *ZFP36L2*. The sequencing results were then used to select potential gRNAs that flank SpCas9's PAM sequence. After 12 potential gRNAs were selected, Cas-OFFinder was used to align the gRNA sequences to the human genome (Bae, 2014). Cas-OFFinder only considers alignments to sequences that flank the SpCas9's PAM sequences, 5'-NGG-3'. In addition to the desired alignment of the *ZFP36L2*, Cas-OFFinder displayed alignments that had up to 3 mismatches. All gRNAs that had non-target alignments to other parts of the genome without at least one mismatch in the seed region of the off-target genomic region was ruled out as non-specific gRNAs. The gRNAs that had no non-target alignments or non-target alignments with at least one mismatch in the seed region of the off-target genomic region were kept as suitable gRNAs for *ZFP36L2*. Six total gRNAs were ruled out because of the Cas-OFFinder alignment results. Six sequences were determined to be suitable and a summary of them can be found in **Table 1**. For increased confidence, on-target and off-target scores were generated using the Doench and Hsu methods (Doench, 2016) (Hsu, 2013). The selected six SpCas9 gRNAs were cloned into a pUC19 vector and simultaneously transfected alongside the SpCas9-encoding pX459 vector to screen whether if they can induce mutations in *ZFP36L2* gene. Afterward, genomic DNA was

extracted for each condition and the cut site for each guide was amplified in PCR using primer pairs that spanned less than 500 bp of the target cut site. The amplicons were run on a 4% agarose gel and the gel image was imported into ImageJ to analyze for small bands or smearing that indicated the presence of a mutation. From the analysis, genomic DNA from samples of promoter guide, TAAACAGGGCTTGAGCGCCG, and the exonic guide, GGTCCGACAGCGAGTCCGGG, had faint, shorter bands in the PCR, indicating that the gRNAs induced a mutation. These two gRNAs were selected as the top candidates for the two-gRNA induced mutation of *ZFP36L2* in HeLa cells.

Table 1: Information on the six gRNAs cloned targeting *ZFP36L2*'s genomic sequence. Columns 1-8 are the Cas-OFFinder results. Columns 9-10 are the On-Target and Off-Target scores generated by Benchling molecular biology tools.

Region	Strand	gRNA sequence (non-comp)	PAM	# of 2/3-nt mismatches	# of 2/3-nt mismatches in seed region (10bp of 3' end of genome sequence)	# of 3-nt mismatches NOT IN seed region (10bp of 3' end of genome sequence)	Ideal?	On-Target Score (Doench et al., 2016)	Off-Target Score (Hsu et al., 2013)
Promoter	+	TAAACAGGGCTTGAGCGCCG	GGG	2	2	0	Yes	67.3	48.5
Promoter	-	CGGCCACGCTAAACGTACCG	GGG	0	0	0	Yes	68.8	49.7
Promoter	+	GAATATCGCAACCATCCCCG	CGG	0	0	0	Yes	73.6	48.8
Exon	-	GGTCCGACAGCGAGTCCGGG	GGG	3	3	0	Yes	70.8	87.8
Exon	+	GACCGCGACAGCTACCTAAG	CGG	0	0	0	Yes	70.3	48.0
Exon	-	AGCCGCTTAGGTAGCTGTCG	CGG	5	5	0	Somewhat yes	65.6	46.9

Kill curve for puromycin selection in HeLa cells

To deliver our gRNAs and necessary proteins inside the cell for the knockout event to take place, plasmid vectors were used with lipid nanoparticles to deliver constructs past the cell membrane and into the cytosol. pX459 was the vector used to transfected HeLa with Cas9, the endonuclease used to induce the double stranded break in the DNA. Encoded in the pX459 vector is a puromycin resistance gene, which allows selection for

cells that uptake the plasmid into their nucleus and are actively transcribing the genes it contains. To maximize efficiency in selecting mutated clones, a kill curve was done on HeLa cells to determine the lowest concentration of puromycin needed to cause a substantial kill-off of non-resistant HeLa cells. HeLa cells were incubated with varying concentrations of puromycin and cultured for 72 hours. Every 24 hours, a viability reading was taken to determine the relative population of viable cells in each condition. The results can be found in **Figure 2**. Based on these results, 0.5 ug/mL was determined to be the lowest effective concentration of puromycin, which causes a greater than 60% kill-off of HeLa cells.

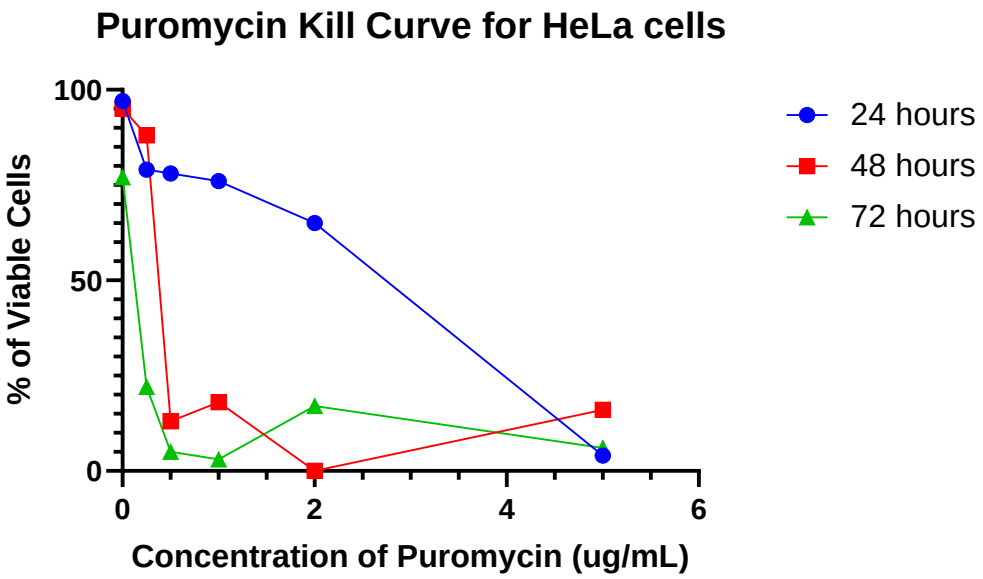

Figure 2: Puromycin kill curve for HeLa cells. HeLa cells were treated for various concentrations of puromycin (0.25, 0.5, 1, 2, and 5 ug/mL) and cultured for 72 hours. Timepoints were taken at 24, 48, and 72 hours to determine viability of cells.

Screening for *Zfp36l2* knockout HeLa populations

To develop a HeLa cell line with *ZFP36L2* expression stably downregulated, a Cas9 encoding vector, pX459, and two gRNA-containing vectors were transfected into wild-type HeLa cells using Lipofectamine 3000. The transfection mixture was incubated for 72 hours, with the last 24 hours being in the presence of the selection marker, puromycin resistance, which is part of the pX459 vector. After the transfection, a subset of the cells was cryopreserved, and the remaining was used for single cell sorting to separate out individual colonies. These colonies were grown initial on a 96-well plate, then expanded to a 24-well plate and prepared for genotyping. To determine which isolated single cell colonies received the desired deletion in HeLa cells, a PCR genomic screen was conducted with 40 isolated clones. The initial PCR screen used primer sets that span most of the genomic sequence of *ZFP36L2*, beginning at the promoter region and ending at the beginning of the 3' UTR. It was anticipated that wildtype genotypes would not produce an amplicon, due to being too large whereas, it was expected that mutant colonies with a deletion in *ZFP36L2* would yield an amplicon due to its shorter sequence. Out of the 40 clones, 19 of them produced a band of the expected size of 290 basepairs, which is approximately the expected size if the complete deletion took place, indicating the presence of a deleted allele. Out of the 19 positive clones, 3 clones were randomly selected for further analysis.

To determine the complete sequence of both alleles present, clones #6, #14, and #15 were used for sequential PCR analysis. The PCR amplicons produced from a pair of *ZFP36L2* -spanning primers were Sanger sequenced. Clones #6 and #15 were found to be identical. Both had a deletion that stretched from the promoter gRNA-binding site to

the exonic gRNA-binding site resulting in an amplicon of 290 basepairs. On the other hand, clone #14's sequencing results produced three separate bands. The first band was 290 basepairs long and identical to the NHEJ event in clones #6 and #15, where the entire coding sequence of *ZFP36L2* was deleted. The second band was 504 basepairs long and represented two recombination events, the first being in the promoter region, adjacent to the promoter gRNA-binding site. The second deletion was found adjacent to the exonic gRNA-binding site and stretched upstream to the first exon. The third band from colony #14 was ~600-700 basepairs long but was unable to be sequenced due to low yield from gel extraction and poor readings from sanger sequencing. These results suggested that at least two separate knockout events took place, one of which being the expected event where the entire coding sequence of *ZFL36L2 was* deleted. These results do not rule out the possibility that a wild type *ZFP36L2* allele may still be present, because the wildtype band is not detectable in PCR using the same primer pairs, due to the long length of the amplicon in wild type.

Next, to determine homogeneity between both alleles, a longer primer pair that spans the entire *ZFP36L2* gene was ran in PCR for clones #14 and #15. A robust Q5 polymerase, which can amplify the wild-type *ZFP36L2* amplicon, in addition to the truncated alleles was used in this screen. Clone #6 was excluded from the proceeding experiments due to having identical results as clone #15 in the previous PCR screen. Both clones #14 and #15 yielded the original truncated band of the single recombination event, indicating at least one allele in the clones had a large deletion in the *ZFP36L2* gene. They also yielded another pair of identical bands that were ~300 base pairs smaller than the wild-type control. This discrepancy was found by Sanger sequencing to be due

to a single deletion in the promoter region of *ZFP36L2*. For clone #14, two additional bands were also found that corresponded to bands two and three, described in the previous paragraph. It is unclear why four bands were present in clone #14 but it is suspected to be due to a non-homogenous population of cells, due to two or more cells mistakenly loaded into the same well during single cell sorting.

In summary, out of the 40 total clones screened in the initial round of genotyping, 3 were selected to be moved forward with. A graphic representation of the three genomic screens can be found in **Figure 3**. Clone #6 was confirmed to be a heterozygous clone with one allele containing one large deletion causing the loss of *ZFP36L2* genomic sequence while the second wildtype allele was still present. Clone #15 was confirmed to be a heterozygous clone as well, with one allele containing a large deletion causing the loss of *ZFP36L2's* genomic sequence. Clone #15's second allele was observed to have a complete ORF while having a truncated promoter region adjacent to the promoter gRNA-site. Clone #14 was observed to have the same genotype as clone #15, however, it has an unexpected allele that consists of two different deletions mediated by both the promoter and exonic gRNA-sites independently with independent NHEJ events. It is suspected that the presence of multiple alleles is

due to the presence of multiple clones, likely due to two or more single cells being loaded into the same well during single cell sorting.

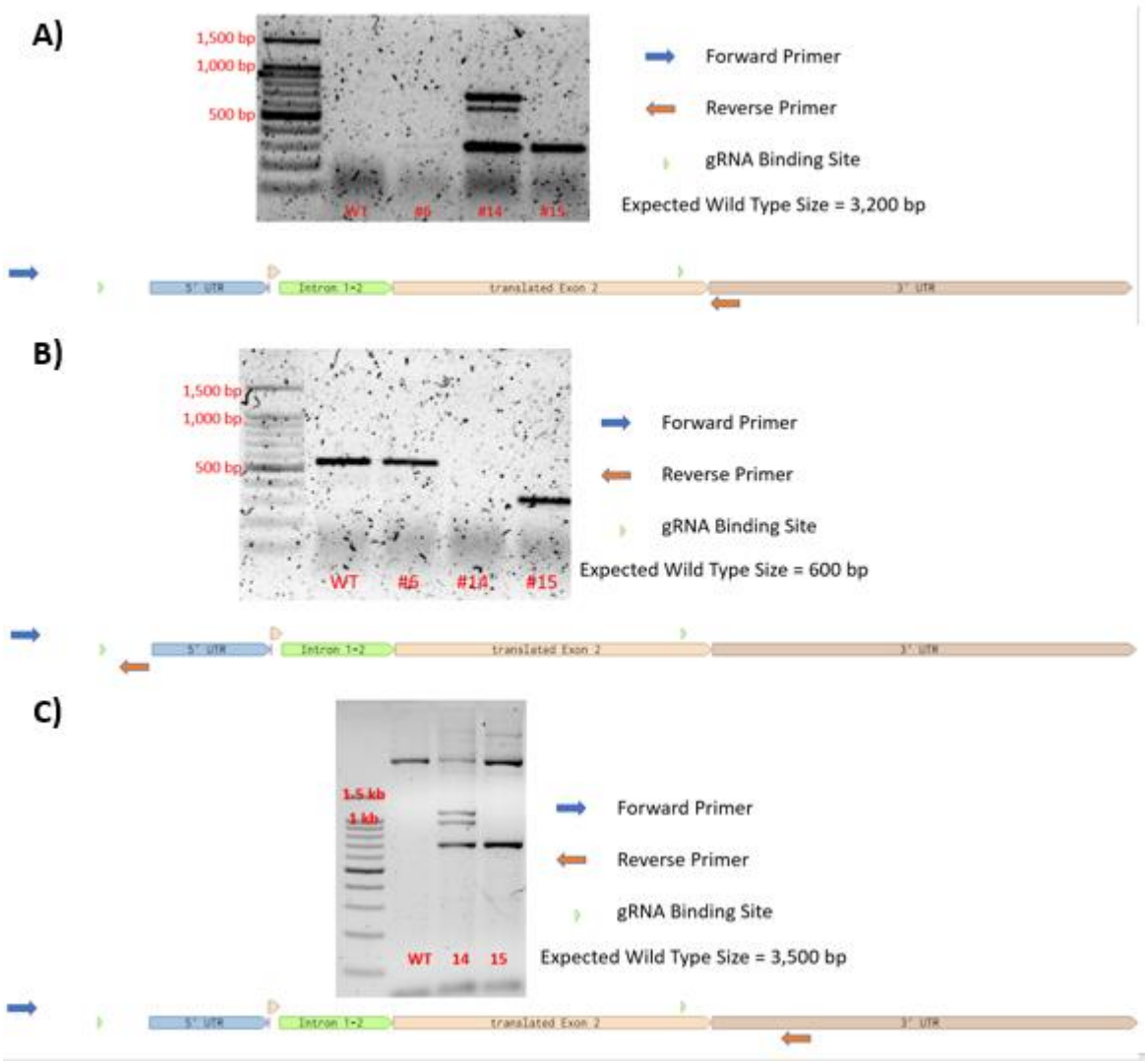

Figure 3: PCR results from genotype ZFP36L2 knockout colonies. A) *ZFP36L2*-spanning PCR results using GoTaq polymerase. **B**) PCR results spanning the promoter region of *ZFP36L2*. **C)** PCR results for the extended *ZFP36L2*-spanning primer pair using Q5 polymerase.

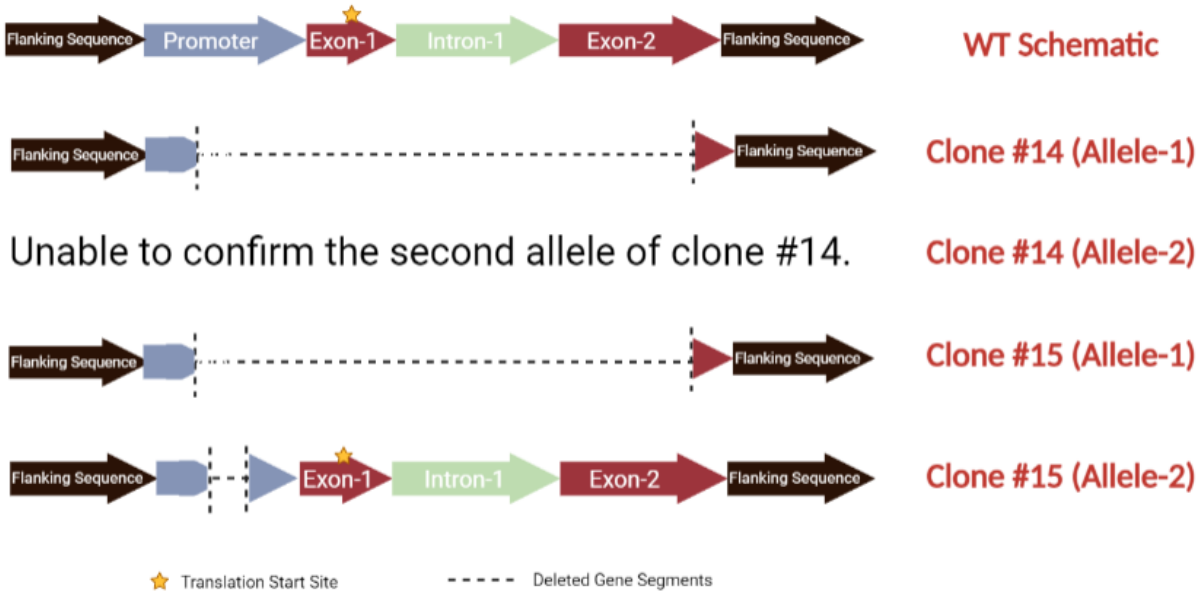

Figure 4: Summary of genotyping results for *ZFP36L2* knockout clones #14 and #15. A) Wildtype schematic of *ZFP36L2*. **B)** Allele-1 for clone #14. **C)** Allele-2 for clone #14**. D)** Allele-1 for clone #15. **E)** Allele-2 for clone #15

Assessing *Zfp36l2* expression post-knockout using CRISPR-Cas9

Given that the two clones isolated were observed to be heterozygous knockouts of *ZFP36L2*, RT-Qpcr was conducted to determine the relative expression of *ZFP36L2* Mrna in the knockout clones #14 and #15, relative to the parent wild type HeLa cells. The results can be found in **Figure 5**. Across two separate biological trials with three technical replicates, *ZFP36L2* Mrna was found to be downregulated with a pooled average of 82% and 78% in clones #14 and #15, respectively. These results indicate that the loss of one functional allele is enough to cause a greater than 2-fold reduction in steady state Mrna expression levels. It is worth mentoning that Mrna transcript levels do not always correlate

to functional protein levels. Multiple attempts were taken to visualize changes in ZFP36L2 protein levels using western blotting. However, the attempts were unsuccessful to generate protein bands corresponding to the correct size of ZFP36L2 protein. Although Mrna levels indicate *ZFP36L2* transcripts were significantly donwregulated, this finding cannot be conclusively until protein levels are observed.

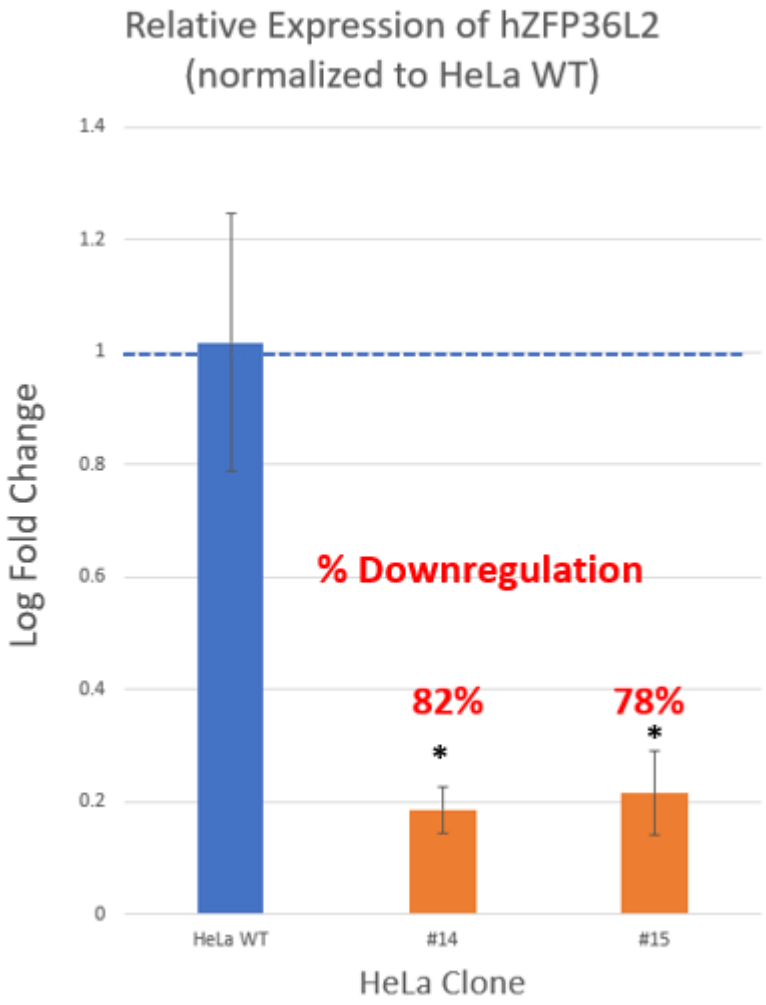

Figure 5: RT-qPCR results for *ZFP36L2* in clones #14 and #15, relative to the wildtype. Relative expression of *ZFP36L2* to wildtype, normalized to GAPDH expression. *p<0.05

Many KDM mRNAs have 3' UTR AREs and are potential targets for ARE-mediated decay

Research from our laboratory indicates that various histone lysine demethylases may be decay targets of ZFP36L2 (Dumdie, 2021). To predict the likelihood of ZFP36L2 targeting KDMs for decay, a program called AREScore was used to determine a predictive score for KDMs with AREs in their 3' UTR (Spasic, 2012). Using the software's online server, all KDMs were queried and computed a score based on the number of AUUUA pentamers they contained in their 3' UTR, their proximity to each other, and the relative AU content that surround them. 22 known KDMs were queried, four of which resulted in a score of 0, indicating that they do not have an ARE in their 3' UTR. The rest of the genes received a score. A graphical representation of KDMs and there AREScores can be found in **Figure 6**. The top four scoring genes were *KDM7A*, which had the highest score of 31.45, *KDM5A*, which had a score of 19.85, *KDM1B*, which had a score of 15.3, and *KDM5B*, which had a score of 12.4. Three of the top four scoring KDMs (*KDM1B, KDM5A, KDM5B*) were previously also shown to be significantly deregulated in *ZFP36L2* knocked-out mice and knocked-down HeLa cells (Dumdie et al). The remaining 18 KDMs had received an AREScore of between 1 and 10. A score of 1, indicates that the gene has a single ARE. As described by the authors (Spasic, 2012), genes with AREScores >3.9 had a 53% rate for true positives. Given these results, AREScores >4 was used as the cutoff for significant AREScore levels. AREScores <4 do not necessarily mean the genes do not have AREs but rather they might not be major ARE-mediated decay targets.

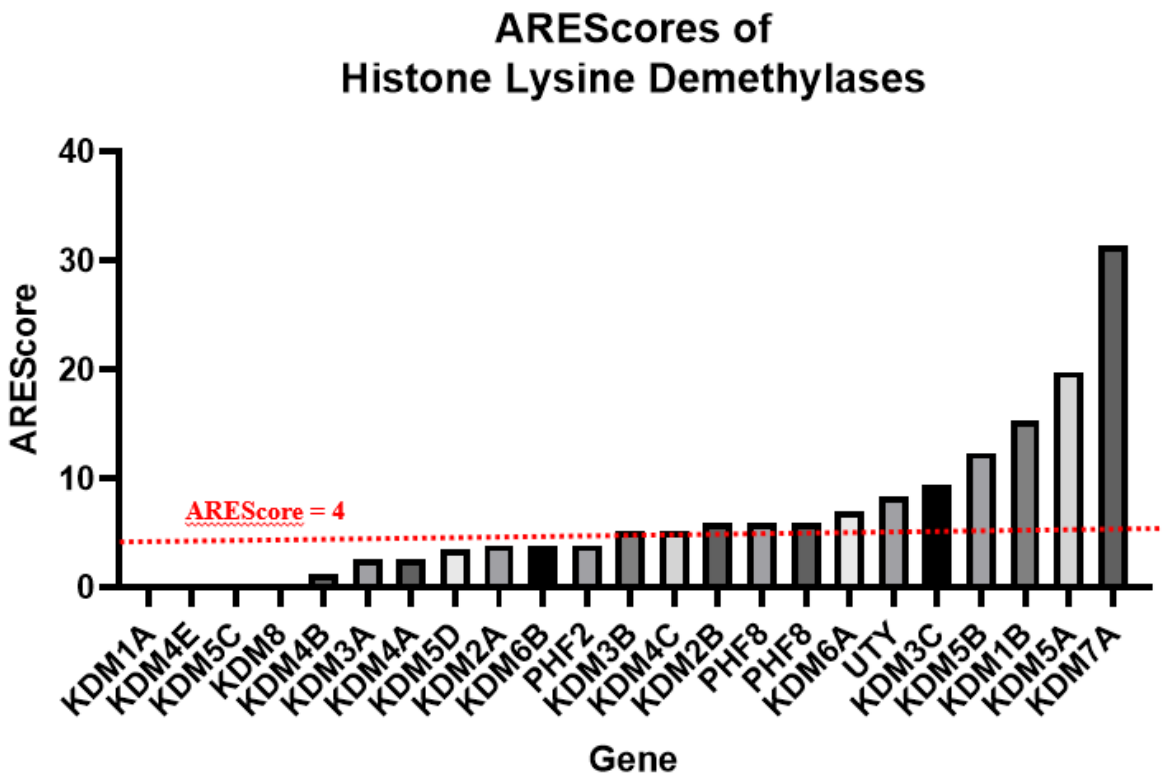

Figure 6: AREScores for histone lysine demethylases. All know KDMs were inputted and queried using the ARE Scorer. (Spasic, 2012)

Effects of heterozygous knockout of *ZFP36L2* on KDM mRNA levels

It was hypothesized in the design of the study that the downregulation of ZFP36L2 will result in an increase in the stability of KDM mRNAs with AREs in their 3' UTRs, which might be reflected by a detectable increase in steady-state mRNA levels. RT-qPCR was performed to assess mRNA expression of *KDM1B, KDM4B, KDM4C, KDM5A,* and *KDM5B*. The results are displayed in **Figure 7**. Comparing the relative expression to wild type in two biological trials with three technical replicates each, In heLa clones #14 and #15 had 51% and 30% less expression of *KDM1B*, respectively. For *KDM4B*, clones #14

and #15 had 56%and 21% less expression, respectively. For *KDM4C*, clones #14 and #15 had 48% and 55% less expression, respectively. For *KDM5A*, clones #14 and #15 had 10% and 2% less expression, respectively. For *KDM5B*, clone #14 had 75% less expression but clone #15 had 8% more expression, relative to the wildtype. To conclude, clone #14 had significant ($p<0.05$) downregulation of *KDM1B* (AREScore = 15.3), *KDM4B* (AREScore = 1.3), *KDM4C* (AREScore = 5.2) and *KDM5B* (AREScore = 12.4). Clone #15 had significant downregulation of *KDM1B*, *KDM4B*, and *KDM4C*. None of the KDMs screening showed consistent upregulation at the steady-state level, contrary to our hypothesis.

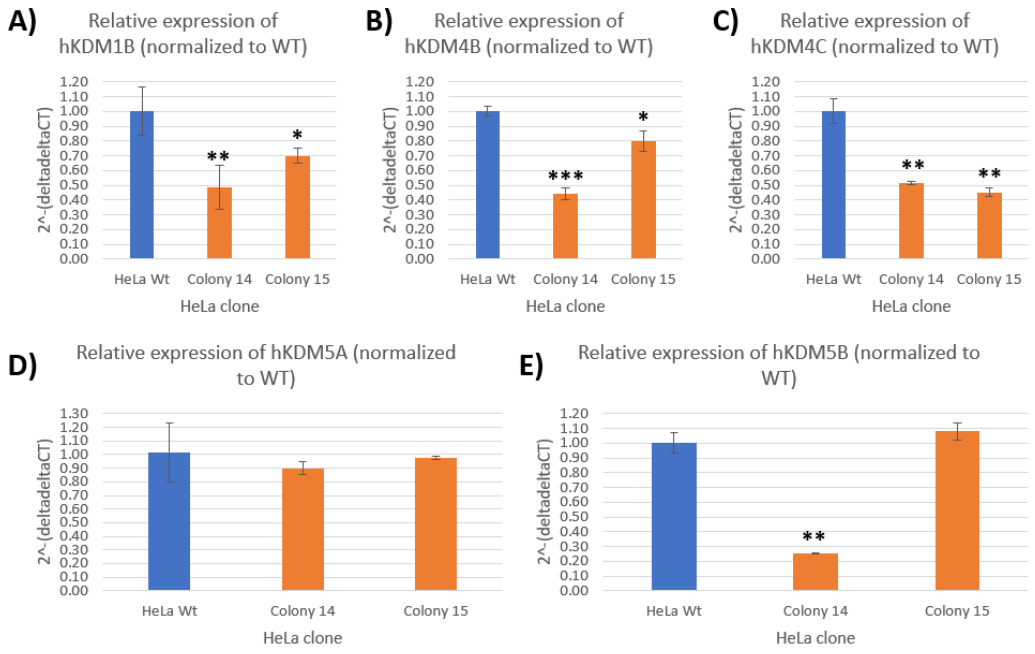

Figure *7*: **RT-qPCR results for KDMs in clones #14 and #15, relative to the wildtype and normalized to GAPDH expression. A)** KDM1B. **B)** KDM4B. **C)** KDM4C. **D)** KDM5B. **E)** KDM5C. *p<0.05, **p<0.01, ***p<0.001

Effects of heterozygous knockout of ZFP36L2 on cell proliferation

It has been previously reported that the loss of or downregulation of ZFP36L2 can inhibit cell proliferation (Suk,2018) (Liu, 2018) Whether proliferation is increased or decreased is largely dependent on the cell type in question. To address this question in HeLa cells, a cell count assay as well as an alamarBlue cell proliferation assay was run on the HeLa clones #14 and #15 and compared to wild type. For the cell count assay, an equal number of cells from each clone was plated on a 24-well plate. Cell counts were taken every 24 hours using tryphan blue staining solution and an automated cell counter. Relative to wild type, colonies #14 and #15 had 61% and 28% less cells at 24 hours, respectively. At 48 hours, they had 61% ($p = 0.01$) and 23% less compared to wild type, respectively. At 72 hours, they had 16% and 2% less cells compared to wild type, respectively.

The alamarBlue cell proliferation assay measures cell proliferation through measuring metabolic oxidation levels, which have been showed to correlate to proliferative rate. For the alamarBlue assay, an equal number of cells was plated for each variant in a 96-well plate. Every 24 hours, measurements of metabolic activity were measured and quantified via spectrophotometry using a color-changing metabolic indicator called Resazurin. In comparison to the wild type, HeLa clone #14 was between 35% to 50% as proliferative as the wildtype. On the other hand, clone #15 displayed a similar rate of proliferation to wild type. Relative to the wildtype, both clones #14 and #15

were less proliferative in the first 48 hours but increased in proliferative rate between 48 and 96 hours.

In conclusion, HeLa clone #14 might be less proliferation than the wildtype, however, colony #15 appears to be comparable to the wildtype in terms of proliferative rate. The cell count assay displayed similar conclusions as the alamarBlue assay with clone #14 having lower cell counts relative to both clone #15 and the wildtype. Significant differences were only found when comparing the cell counts of colony #14 to wild type at the 48-hour timepoint. A 96-hour checkpoint was not done for these cells because of over confluency in the wells. Significance for the alamarBlue was only found when comparing wild type to colony #14, which had p-values< 6E-08, 5E-06, 0.005, and 0.005 corresponding to timepoints at 24, 48, 72, and 96 hours, respectively.

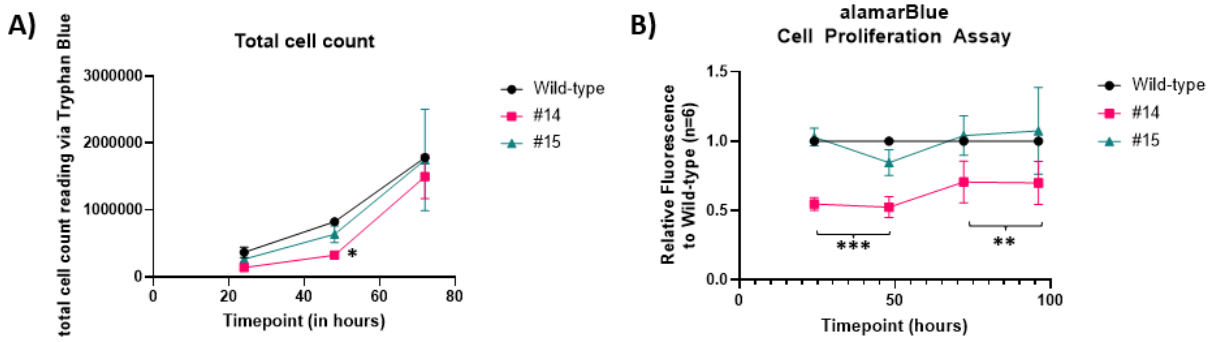

Figure 8: Cell proliferation assays comparing *ZFP36L2* knockout clones #14 and #15 to wildtype. A) alamarBlue metabolic-based proliferation assay **B)** Total cell count assay. *p<0.05

Computational analysis of gene stability in RNA-seq data from *ZFP36L2* knocked out MOLM-13 cells

To assess the change in transcriptomic stability due to homozygous knockout of *ZFP36L2* in a different cancer cell model, a published algorithm, exon-intron splice analysis (EISA), was used to analyze RNA-seq data previously published by Wang et al (2021). Wang et al developed the CRISPR-Cas9 mediated *ZFP36L2* knockout variant in MOLM-13, a widely utilized AML-modeling cell line. The authors developed replicates of *ZFP36L2*(-/-) clones using two different gRNAs. For reference, these clones are referred to as dataset-1 and dataset-2 clones. The control datasets used in this study were wild-type MOLM-13 cells, introduced to scrambled gRNA sequences that have no alignment to the human genome. These datasets were assessed for changes in mRNA stability using a previously published bioinformatic pipeline, EISA, that determines stability by assessing changes in total read counts of intronic and exonic genes (Gaidatzis, 2015). The pipeline considers genes to be significantly stabilized if total intronic counts decreased in the test condition, relative to the control, and total exonic counts increased. Additionally, genes that had an increase in total intronic counts and decrease in total exonic counts are considered to destabilized. Although relatively few genes showed a difference in stability, a greater proportion of genes were predicted to have increased stability in the absence of *ZFP36L2* relative to the wild-type control in both datasets. For dataset 1, 16 genes significantly gained stability, and 8 genes significantly lost stability. For dataset 2, 15 genes significantly gained stability, and 5 genes significantly lost stability. Several genes were found to be overlapped across both datasets. Across both datasets, six genes were significantly increased in stability and 3 genes were significantly

decreased in stability. *FN1* was found to be the most significantly stabilized gene across both dataset-1 and dataset-2 with an FDR value of 7.83x10-11 and 1.12x10-10, respectively. FN1 is an important extracellular matrix protein that has been associated with multiple different types of cancers, including gastric cancer (high expression of fibronectin 1 indicates poor prognosis in gastric cancer). Additionally, *WDR83, ACTA2, ADGRE3, NWD1, and FOSL2* were found to be significantly stabilized across both datasets. On the other hand, three genes were simultaneously found to be significantly destabilized across both datasets, including *CTBP1*, *MCM3AP-AS1*, and *SETD9T*. A notable chromatin modifier that was found to be significantly stabilized exclusively in dataset-2 is histone deacetylase 2, which is associated with decreased transcription due to inducing chromatin condensation. A summary of all significant genes from the stability analysis can be found in Tables 2 and 3. To determine if any of the genes that were found to be significant contain AREs in the 3' UTR, the AU-Rich database was used (Fallmann, 2015). It was found that out of the 10 genes that were found to be either stabilized or destabilized across both datasets, only *FN1* and *FOSL2* contained ARE elements in their 3' UTR. Although the gene lists generated from this analysis did not indicate KDMs to

being significantly destabilized, these lists do provide potential leads to investigate to find potential associations that contribute to ZFP36L2's role in AML.

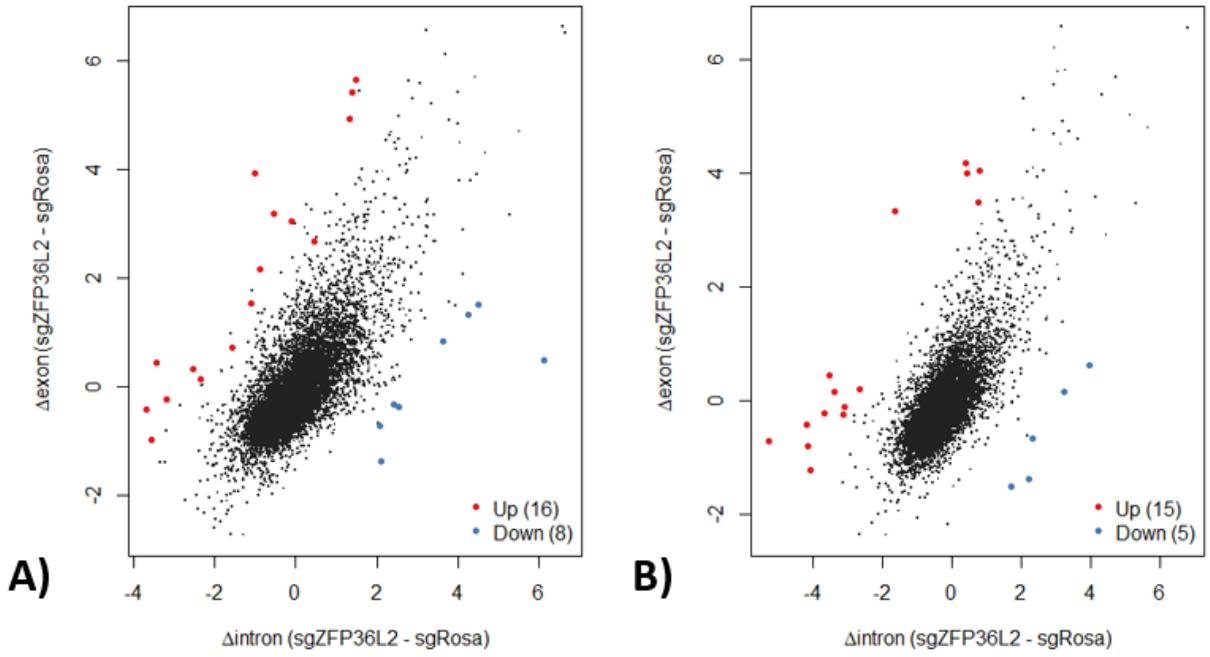

Figure 9: Post-transcriptional decay normalization of RNA-seq data from *ZFP36L2*(-/-) MOLM-13 cells. A) Comparison of gRNA-1 for *ZFP36L2* against non-targeting gRNA control. **B)** Comparison of gRNA-2 for *ZFP36L2* against non-targeting gRNA control. Red = genes with increased stability. Blue = genes with decreased stability. Significance was set at $p<0.05$

Table 2: List of significant genes found from the comparison of gRNA-1 for *ZFP36L2* against non-targeting gRNA control.

Database-1				
Genes with Increased Stability				
Gene Symbol	**Gene Name**	**Gene Function**	**FDR**	**LOG Fold Change**
FN1	Fibronectin-1	Cell adhesion and migration	7.83E-11	5.0885
WDR83	WD Repeat Domain 83	Molecular scaffold, promotes ERK signaling	1.88E-06	7.6828
ACTA2	Actin Alpha 2	Smooth muscle actin, vascular contractility, and blood pressure homeostasis	0.000228	6.7723
CSMD1	CUB and Sushi Multiple Domains 1	Involved in memory and reproductive structure formation	0.00029	3.0008
ADGRE3	Adhesion G Protein-Coupled Receptor E3	Transmembrane receptor largely found in immune cells	0.001224	4.0113
NWD1	NACHT And WD Repeat Domain Containing 1	Modulation of androgen receptor activity	0.001374	4.8979
PABIR3	PABIR Family Member 3	Serine, threonine phosphatase inhibitor	0.004204	2.7093
GTDC1	Glycosyltransferase Like Domain Containing 1	glycosyltransferase activity	0.004942	3.3694

Table 2: List of significant genes found from the comparison of gRNA-1 for ZFP36L2 against non-targeting gRNA control, Continued

CAVIN1	Caveolae Associated Protein 1	Regulates formation of pre-rRNA complex	0.004975	7.6698
C15orf61	Chromosome 15 open reading frame 61	Uncharacterized	0.010137	2.3981
CLEC4A	C-Type Lectin Domain Family 4 Member A	Cell adhesion, cell signaling and immune response	0.017312	4.6498
RAPH1	Ras Association (RalGDS/AF-6)	Cell migration and actin network assembly	0.017312	2.7824

Table 2: List of Significant Genes in Dataset 1, Continued

CREB5	CAMP Responsive Element Binding Protein 5	Trans-activator of cAMP production	0.026446	4.5318
AQP9	Aquaporin 9	Membrane permeability factor, specialized to leukocytes	0.028924	5.3522
FOSL2	FOS Like 2, AP-1 Transcription Factor Subunit	Subunit of a transcription factor	0.028924	4.5031
VPS9D1	VPS9 Domain Containing 1	GTPase activator activity	0.028924	2.3245

Genes with Decreased Stability

Gene Symbol	Gene Name	Gene Function	FDR	LOG Fold Change
CTBP1	C-Terminal Binding Protein 1	Transcriptional repressor	5.83E-09	-9.6043

Table 2: List of significant genes found from the comparison of gRNA-1 for ZFP36L2 against non-targeting gRNA control, Continued

MCM3AP-AS1	MCM3AP Antisense RNA 1	lncRNA that is developing as a cancer indicator	0.001374	-7.2385
NCF1	Neutrophil Cytosolic Factor 1	Production of superoxide anions	0.00515	-3.9046
S100A9	S100 calcium binding protein A9	Cell progression and differentiation	0.005926	-4.5466
CRBN	Cereblon	Protease, involved in brain development	0.014422	-6.6802
SETD9	SET Domain Containing 9	Enables lysine N-methyltransferase activity	0.026446	-3.6718
ZNF224	Zinc Finger Protein 224	Coactivator of Wilm's tumor protein 1, a leukemia marker	0.026446	-6.4633
CTSD	Cathepsin D	Protein turnover and protolytic activation of hormones and growth factors	0.048438	-2.9281

Table 3: List of significant genes found from the comparison of gRNA-2 for *ZFP36L2* against non-targeting gRNA control.

Database-2				
Genes with Increased Stability				
Continued				
Gene Symbol	**Gene Name**	**Gene Function**	**FDR**	**LOG Fold Change**
FN1	Fibronectin-1	Cell adhesion and migration	1.12E-10	5.1692
BDNF-AS	BDNF antisense RNA	Degradation of the brain-derived neurotrophic factor	4.00E-05	6.1672
WDR83	WD Repeat Domain 83	Promotes ERK Signaling	4.00E-05	7.3375
HDAC2	Histone Deacetylase 2	Deacetylation of lysine residues on the core histones H2A, H2B, H3, and H4	4.00E-05	8.501
ACTA2	Actin Alpha 2	Smooth muscle actin, vascular contractility and blood pressure homeostasis	0.000349	6.7618
ADGRE3	Adhesion G Protein-Coupled Receptor E3	Transmembrane receptor largely found in immune cells	0.000816	4.0732
C12orf29	Chromosome 12 open reading frame 29	Uncharacterized	0.003382	6.6792

Table 3: List of significant genes found from the comparison of gRNA-2 for ZFP36L2 against non-targeting gRNA control, Continued

YWHAH	Tyrosine 3-Monooxygenase/Tryptophan 5-monooxygenase Activation Protein	Mediation of signal transduction	0.003382	7.192
Continued				
SIK3	SIK Family Kinase 3	Phosphorylates serine/threonine residues and facilitates TORC1 and TORC2 signaling	0.00442	7.2373
SPIRE1	Spire Type Actin Nucleation Factor 1	Actin organization	0.008733	4.2846
TTC39B	Tetratriopeptide Repeat Domain 39B	Cholesterol homeostasis	0.008733	7.5716
CCDC50	Coiled-Coil Domain Containing 50	Suppressor of EGFR	0.009869	4.3493
FOSL2	FOS Like 2, AP-1 Transcription Factor Subunit	Subunit of a transcription factor	0.010817	7.5847
RIN2			0.011972	2.8634
NWD1	NACHT And WD Repeat Domain Containing 1	Modulation of androgen receptor activity	0.019345	4.1864

Table 3: List of significant genes found from the comparison of gRNA-2 for ZFP36L2 against non-targeting gRNA control, Continued

Genes with Decreased Stability				
Gene Symbol	**Gene Name**	**Gene Function**	**FDR**	**LOG Fold Change**
ATP6V1C2	ATPase H+ Transporting V1 Subunit C2	Subunit of V-ATPase, contributes to organelle acidification	0.000816	-7.383
Continued				
MCM3AP-AS1	MCM3AP Antisense RNA	lncRNA that is developing as a cancer indicator	0.007203	-6.876
SETD9	SET Domain Containing 9	Enables lysine N-methyltransferase activity	0.009643	-3.981
CTBP1	C-Terminal Binding Protein 1	Transcriptional repressor	0.015557	-7.184
ERCC1	Endonuclease Non-Catalytic Subunit	Subunit in DNA lesion repair pathways	0.019685	-6.906

Conclusions

In conclusion, the purpose of this project was to expand upon the findings of Dumdie et al to determine if ZFP36L2's role in deregulating the expression of KDMs have an effect on the proliferative rate of cells. More specifically, the first aim of this study was to determine if *ZFP36L2* acts in HeLa cells to degrade KDM mRNAs, thus regulating their expression. Inconsistent with what was found in Dumdie et al, stable downregulation of *ZFP36L2* resulted in the downregulation of relative transcript levels for various KDMs that were previously found to be stabilized due to *ZFP36L2* loss of function. These results were true for *KDM1B*, *KDM4B*, and *KDM4C*, however, it is worth noting these results were only true for KDM steady-state transcript levels and the effects on mRNA stability were not determined by decay assays. The second aim of this project was to determine if downregulation of *ZFP36L2* induces a change in cell proliferation of HeLa cells. The results indicated that one of two stable heterozygous knockouts had slightly lower proliferation. However, because these results were not consistent in both clones or at all timepoints measured in the experiment, further investigation will be required to determine whether there is an association between *ZFP36L2* expression and cell proliferation. The last aim of the study was to computationally investigate whether the loss of *ZFP36L2* causes deregulation of KDM transcripts in another cancer cell line modeling acute myeloid leukemia. To address this question, previously published *ZFP36L2*$^{(-/-)}$ MOLM-13 RNA-seq data was analyzed using a method called EISA to assess mRNA stability. A surprisingly small number of mRNAs were found to have altered.

Although these results indicate that there is a relationship between *ZFP36L2* activity and KDM transcript levels, further studies are required to solidify and

better understand the mechanistic relationship between stable knockdown or knockout of *ZFP36L2* and KDM mRNA targets.

Discussion

ZFP36L2 is a therapeutic target that has gained more and more attention in recent times. It has been indicated as a major target for a vast array of both solid and liquid tumors (Suk, 2018) (Liu, 2018). Despite these associations, a great number of questions remain regarding the role of *ZFP36L2* in the onset and/or progression of cancer. Prior research and data suggest that *ZFP36L2* generally acts as a tumor suppresspr. For example, Suk et al. showed that in colorectal cancer, overexpression of *ZFP36L2* inhibits cell proliferation and promotes cell cycle arrest by downregulating cyclin D, a major checkpoint protein in the cell cycle (Suk, 2018). Liu et al. showed that in AML, overexpression of *ZFP36L2* inhibits cell proliferation, promotes differentiation, and cell cycle arrest at the G0/G1 cell cycle stage (Liu, 2018). It was inferred that this role of *ZFP36L2* was due to it being a major regulator of KDM expression, which are common chromatin modifying proteins that are often found to be deregulated in cancer (Sterling, 2021).

Although I set out to make a homozygous knockout of *ZFP36L2,* I only found heterozygous knockouts in my screen. This might be because of a few different reasons. The first reason why a homozygous knockout was not obtained is because I did not screen the different clones extensively enough. After the original screen I did with the 40 clones and after selecting clones #6, #14, and #15, I did not cryopreserve or maintain the culture of the other clones found to have mutations in my initial genotyping screen. Additionally, I did not realize the possibility of CRISPR-Cas9 deletion to only take place in one allele and was not able to confirm this until months after troubleshooting, till Q5 polymerase was used as a method to be able to amplify the entire length of ZFP36L2's

genomic region. Another possibility of why no homozygous knockouts were able to be obtained after sorting is that ZFP36L2 may be an essential gene in HeLa cell. Out of the 288 single cell colonies that were sorted, only 40 survived to be transferred to a 24-well plate for genotyping. An explanation for this may be that the colonies that died may potentially have been homozygous knockouts.

The results obtained from this study with heterozygous knockout of *ZFP36L2* are not consistent with the original hypothesis. The genomic screens of HeLa clones #14 and #15 clearly showed the presence of one allele with the coding sequence of *ZFP36L2* deleted. This resulted in a greater than 75% reduction of *ZFP36L2* transcript levels. Although these results suggest that ZFP36L*2* levels might be reduced, Western blots will need to be done on these clones to ask whether this mutation significantly reduced levels of ZFP36L2 protein. In addition to protein level, the phosphorylation of ZFP36L2 is important to consider as these modifications have previously been described to play an role in regulating the protein's localization and activity (Adachi, 2014), (Wang, (2015)).

These clones were also assessed for cell proliferation and found too potentially be less proliferative. These findings were inconsistent with our hypothesis, which was that knockdown of *ZFP36L2* would increase cell proliferation. This inconsistency may be due to potential compensatory mechanisms that helped mitigate the loss of ZFP36L2 expression. Another potential explanation is that although *ZFP36L2* mRNA was downregulation, protein levels of ZFP36L2 did not change and protein levels stayed consistent between the wild type and knockout clones. Both clones #14 and #15 trended towards having lower proliferation rates but the only significance was found in the cell count assay, comparing wild type and colony #14 at the 48-hour timepoint. These

experiments will need to be repeated or more sensitive cell proliferation assay will need to be ran to test the relationship more rigorously between ZFP36L2 and cell proliferation and more confidently conclude whether ZFP36L2 is playing a proto-oncogenic role in cancer or a tumor suppressive role.

In addition, select KDMs were found to be downregulated by more than 50% in these clones. In this regard, a factor worth noting is that *ZFP36L2* also contains an ARE in its 3' UTR. By downregulating the expression of *ZFP36L2,* it is possible to increase its stability—and potentially, its expression--by decreasing the post-transcriptional decay of its mRNA. This might be expected to increase the stability and half-life of its mRNA, which increases its potential to locate and decay other downstream targets. This could explain the findings that KDMs, which are anticipated to be direct targets of ZFP36L2, decrease in transcript levels despite the fact the ZFP36L2 expression was downregulated. Because of this, it is necessary to conduct more research on the stability profile of *ZFP36L2* and its downstream targets. In addition, it is also possible that knockdown of ZFP36L2 resulted in a compensatory increase in expression of other activators of ARE-mediated mRNA decay—namely, ZFP36L1 and/or TTP. This would be expected to increase the decay of direct targets of these activators. Since there are many redundancies between the targets of the TTP homologs, homologs of ZFP36L2 may also target KDMs. Thus, increased stability of ZFP36L1 and/or TTP may potentially increase their activity on KDMs and induce their decay more readily, leading to downregulation of their transcript levels.

To assess the role of ZFP36L2 on mRNA stability more directly, it will be critical to use specialized RNA-seq techniques such as SLAM-seq. This is an RNA-seq method that can discriminate between new and old transcripts through the incorporation of the uridine

homolog, 4-thiouridine in newly synthesized mRNAs, which can then be followed over time (Herzog, 2017). By utilizing SLAM-seq, we can look at the overall stability profile of the complete transcriptome in ZFP36L2 depleted cells and determine which mRNAs increase in their half-life. By running SLAM-seq on a ZFP36L2 stably repressed or completely knocked out population of cells, we can expand on the RNA decay assay performed by Dumdie et al and assess stability changes not just in a transient knockout state, but with stable knockout, while screening many more genes (Dumdie, 2018). Analyses such as this will begin to present a more complete picture of the effects of ZFP36L2 on mRNA targets and how they relate to KDM expression and cancer development.

In addition to potential roles for ZFP36L2 in regulation of KDM expression and regulation of cell proliferation, my third hypothesis is that these roles are mechanistically linked. Specifically, I hypothesize that disruption of KDM expression with altered ZFP36L2 expression in cancer cells plays a critical role in cancer cell proliferation and/or survival. In future experiments, this possibility could be tested by developing an inducible overexpression model of ZFP36L2 in cancer cells. By regulating the overexpression of ZFP36L2, we can measure dependencies of the hallmarks of cancer such as cell proliferation and apoptosis as a direct function of upregulating and downregulating ZFP36L2 expression. In addition, if ZFP36L2 is found to regulate histone modifiers in cancer, the effect of such regulation on specific targets can be tested through knockdown and rescue experiments to investigate the possibility of a mechanistic link.

Since the effects of ZFP36L2 deregulation appear to vary significantly between cell types, it is important to test the effects of downregulating Zfp36l2 in a cell line specific

to the cancer type that is being studies, it may potentially be useful to also screen the change in KDM expression in other cell types with ZFP36L2 deregulated to see if there are consistent results with what has been seen here. In addition to downregulation, assessing the effects of overexpression on the hallmarks of cancer and KDM expression will further confirm the findings of this paper or reveal discrepancies. Overexpression may also provide the advantage of increasing sensitivity via inducing a larger change in the relative expression of *ZFP36L2*. This model can be produced by using a lentiviral vector to transduce, integrate, and stably express the ORF of *ZFP36L2*. Additionally, a tetracyclin-inducible promoter can be used alongside the stable expression of a rTet repressor to control the rate of *ZFP36L2* overexpression.

In addition to repeating the experiments assessing the role of ZFP36L2 in cell proliferation, another series of experiments that will provide insight to the role of the ZFP36L2 repression in cancer is to assess markers of apoptosis. Annexin V and flow cytometry can be used to compare the relative percentage of cells that are apoptotic in wild type and ZFP36L2 repressed cells. Additionally, a cell cycle assay can be done to determine difference in what checkpoints ZFP36L2 depleted cells are halted at, relative to wild type. These results will further contribute to determining the effects of ZFP36L2 on another important hallmark of cancer. Lastly, to further assess the therapeutic potential of ZFP36L2 as a cancer target, ZFP36L2 depleted HeLa cells can be treated with common chemotherapies or radiation techniques to assess whether the cells become more or less sensitive to treatment. This will further present helpful information to determine ZFP36L2's role in cancer onset and development.

To conclude, this study assessed the effects of downregulating *ZFP36L2* via CRISPR-Cas9 mediated knockout. Unexpectedly, the results showed specific KDMs were downregulated with stable knockdown, pointing to possible compensatory mechanisms in the cells. I also observed a potential decrease in cell proliferation, which would suggest an oncogenic role for the mRNA decay activator in HeLa cells. However, future research is needed to test these findings more rigorously and to more fully understand the relationship between *ZFP36L2,* regulation of KDM expression and cancer cell proliferation and survival.

Materials and Methods

Cell Culture

The culture of all HeLa cells used in this project was performed in media containing Dulbecco's Modified Eagle Medium (DMEM) supplemented with 10% FBS and 10% anti-mycotic anti-biotic solution on standard tissue culture dishes or plates and incubated at 37 °C with 5% CO_2.

Designing gRNAs to target and knockout ZFP36L2

To design guide RNAs (gRNA) targeting *ZFP36L2*, the genomic sequence surrounding the *ZFP36L2*region needed to be verified for the cell line being used. Online genome mapping tools including Ensembl, UCSC Genome Browser, and Eukaryotic Promoter Database were used to identify the expected genomic sequence of human *ZFP36L2*. From Ensembl, the exonic sequences (coding regions and UTRs) were extracted and uploaded to the annotation software, ApE. Intronic information was extracted from the UCSC Genome Browser, and TSS-flanking sequences corresponding to *ZFP36L2*'s promoter region were extracted using the EPD. All sequences of the *ZFP36L2* genomic region were compiled and annotated onto an ApE entry. Using the entry, primers were designed to PCR amplify desired regions of *ZFP36L2* that would be used for Cas9-mediated mutations. The two regions of interest were the promoter region and the second exonic region of *ZFP36L2*.

Afterward, a DNeasy DNA extraction kit (Qiagen Cat#69504) was used to extract genomic DNA from wildtype HeLa cells. PCR was done using GoTaq polymerase master mix (Promega Cat#M712), primer oligos generated from the ApE file and genomic DNA extracted from HeLa. PCR products were amplified on an agarose gel. The amplified products were gel extracted using a gel purification kit (Qiagen Cat#28104) and sent for sanger sequencing (Genewiz services). The Sanger sequences were aligned to the wildtype sequence to determine the presence of single nucleotide polymorphisms in the *ZFP36L2* gene of the HeLa cell line. Using ApE, gRNA were selected and annotated. A total of 20 guides were originally selected and then computationally screened using CasOFFinder (http://www.rgenome.net/cas-offinder/), which allows for the BLAST alignment of off-target gRNA sequences that are adjacent to a PAM site ('NGG'). Most gRNAs yielded alignments with other regions of the genome with 2-3 mismatched base pairs. The gRNAs that had at least one mismatch in the seeding region of the gRNA, the most crucial part of the gRNA for binding the target sequence, were kept and cloned.

The pUC19 plasmid was used as the donor plasmid for transient expression of the gRNAs in HeLa. First, DNA oligos were ordered for the gRNAs (Table 4). The forward and reverse oligos were ligated together and amplified using the Phusion High Fidelity PCR master mix (New England BioLabs Cat#M0531S), while the pUC19 plasmid was digested using the BamHI restriction enzyme (New England BioLabs Cat#R0136S). The linearized plasmid was purified using Qiagen's PCR purification kit (Qiagen Cat#28104) and the gRNA oligo inserted into the linearize plasmid using Gibson Assembly master mix (New England BioLabs Cat#E2611). The reactions were then transformed into chemically competent DH5alpha E. coli. cells (New England BioLabs Cat#C2987H) and

selected for colonies on ampicillin (+) LB-agar plates for amplification of gRNA expression vectors. Individual colonies were selected and amplified using LB-agar broth and the amplified plasmids were extracted using the Qiagen miniprep kit (Qiagen, Cat#). Insertion of the gRNA sequence into donor plasmids was verified using Sanger sequencing at Genewiz.

Table 4: gRNAs ordered for cloning gRNAs into pUC19

Primer Name	Primer Sequence
gd.L2pF1	TTTCTTGGCTTTATATATCTTGTGGAAAGGACGAAACACCAAACAGG GCTTGAGCGCCG
gd.L2pF2	TTTCTTGGCTTTATATATCTTGTGGAAAGGACGAAACACCGGCCACG CTAAACGTACCG
gd.L2pF3	TTTCTTGGCTTTATATATCTTGTGGAAAGGACGAAACACCAATATCG CAACCATCCCCG
gd.L2eF1	TTTCTTGGCTTTATATATCTTGTGGAAAGGACGAAACACCGTCCGAC AGCGAGTCCGGG
gd.L2eF2	TTTCTTGGCTTTATATATCTTGTGGAAAGGACGAAACACCACCGCGA CAGCTACCTAAG
gd.L2eF3	TTTCTTGGCTTTATATATCTTGTGGAAAGGACGAAACACCGCCGCTT AGGTAGCTGTCG
gd.L2pR1	TCAACTTGCTATGCTGTTTCCAGCATAGCTCTGAAACCGGCGCTCAA GCCCTGTTT
gd.L2pR2	TCAACTTGCTATGCTGTTTCCAGCATAGCTCTGAAACCGGTACGTTT AGCGTGGCC
gd.L2pR3	TCAACTTGCTATGCTGTTTCCAGCATAGCTCTGAAACCGGGGATGGT TGCGATATT
gd.L2eR1	TCAACTTGCTATGCTGTTTCCAGCATAGCTCTGAAACCCCGGACTCG CTGTCGGAC
gd.L2eR2	TCAACTTGCTATGCTGTTTCCAGCATAGCTCTGAAACCTTAGGTAGC TGTCGCGGT
gd.L2eR3	TCAACTTGCTATGCTGTTTCCAGCATAGCTCTGAAACCGACAGCTAC CTAAGCGGC

Scoring adenine-uridine rich elements in KDMs

Scoring adenine-uridine rich elements (ARE) in histone lysine demethylase (KDM) targets was done using the algorithm, AREScore, developed by Spasic et al, PLoS Genet, 2012. AREs are defined as genetic elements that have an enriched concentration of adenine-uridine content. Often, AREs are found in the 3' UTR of mRNA transcripts and have been known to play a role in the stability and decay of transcripts. ARESCore quantifies the potential strength of a gene by assessing the number of occurrences of AUUUA pentamers, their proximity to each other, their surrounding genomic region, and whether they are enriched in AU content. The algorithm first assigns a basal score that is dependent on the number of AUUUA pentamers found in the 3' UTR. Additional points are then added depending on the proximity of the pentamers to each other. Finally, additional points are added to the ARESCore based on the relative enrichment of AU content in the surrounding region of the pentamers.

RNA Extractions and Reverse Transcriptase-Quantitative PCR

Quantification of transcript expression was performed using quantitative reverse transcription-quantitative PCR (RT-qPCR). Cells were detached from culture using 0.05% trypsin and resuspended in Trizol (Invitrogen Cat# 15596026) reagent for RNA extraction. 0.2 mL of chloroform (Sigma-Aldrich, Cat# 288306-100ML) was added to every 1 mL of Trizol. The mixture was vortexed and spun down at maximum speed for 10 minutes. The clear supernatant was then mixed at a 1:1 ratio with 100% ethanol and purified using the Direct-zol RNA miniprep kit (Zymo Research Cat#R2061), according to the

manufacturer's instructions. The isolated RNA samples were quantified and checked for quality using the NanoDrop2000.

RT-qPCR was run in a two-step manner. The first step was synthesizing cDNA using the iScript cDNA synthesis kit (Bio-rad Cat#1708890). For all reactions, between 200 to 1000 ng of total RNA was used for cDNA synthesis. Between 10-25, ng of cDNA was then used for the qPCR reaction. All qPCR reactions were run using the POWER SyBr Green PCR master mix (Applied Biosystems Cat #4368577) on the StepOne qPCR system (Applied Biosystems). All reactions were run with a final primer concentration of 200 nM. The primers used in these experiments were designed to span intronic regions to ensure no genomic amplification took place (Table 5). To normalize for loading variations, hGAPDH primers were run across all samples as an internal housekeeping control.

Table 5: Primers used in RT-qPCR

Primer Name	Primer Sequence
hZFP36L2 qPCR Fwd	TCCAGAAACATGTCGACCAC
hZFP36L2 qPCR Rev	GCATGTTGTTCAGGTTGAGGT
hGAPDH qPCR Fwd	CTGCTCCTCCTGTTCGACAGT
hGAPDH qPCR Rev	ACCTTCCCCATGGTGTCTGA
hKDM1B qPCR Fwd	GGCAAAACCGAACCTAGTCCC
hKDM1B qPCR Rev	TGTGGAGTAAGCTGGATTTCCTT
hKDM4B qPCR Fwd	ACTTCAACAAATACGTGGCCTAC
hKDM4B qPCR Rev	CGATGTCATCATACGTCTGCC
hKDM4C qPCR Fwd	GATGAATGGAACATAGCTCGCC
hKDM4C qPCR Rev	GGTGTGCCATGCAAACGTG
hKDM5A qPCR Fwd	GTCTAAAGTGGGTAGTCGCTTG
hKDM5A qPCR Rev	GTTTGGGTATCAGTGCTGAGAA
hKDM5B qPCR Fwd	GACCCCTTCGCTTTCATCCA
hKDM5B qPCR Rev	TTACACGAGTTTGGGCCTCC

Puromycin Kill Curve

One-hundred thousand HeLa cells were plated in each well of a 24-well plate and cultured until 90% confluent. Puromycin (Sigma-Aldrich, Cat# P9620) was then added to the media at a final concentration of either 0, 0.25, 0.5, 1, 2, or 5 ug/mL. Cells were then cultured for 24, 48, and 72 hours with cell viability being measured using trypan blue staining.

CRISPR-Cas9 Knockout of *ZFP36L2* using a dual sgRNA transfection system

Two-hundred thousand HeLa cells were plated in each well of a 6-well plate and cultured until 90% confluent. The cells were then transfected using Lipofectamine 3000 (Invitrogen #L3000015). Each well was transfected using 1 uL of Lipofectamine 3000, 2 uL of P3000, 0.5 ug of sgRNA_Promoter3 guide plasmid, 0.5 ug of sgRNA_Exon1 guide plasmid, and 0.5 ug of pX459 (Cas9-2A-puro expression vector). After 24 hours, puromycin selection was performed adding a final concentration of 0.5 ug/mL of puromycin to the media. Cells were then cultured for another 48 hours. Viable cells were harvested and transferred to 10 cm plates and grown until ~70 confluent. A subset of cells was cryopreserved. The remaining cells underwent single-cell sorting as described below.

FACS and Knockout Colony Screening

After the *ZFP36L2* mixed-knockout population of HeLa underwent transfection and antibiotic selection, they were sorted into single cell colonies to generate isogenic populations. The HeLa cells were detached from the tissue culture plate using Accutase (Sigma-Aldrich Cat# A694-100ML) and resuspended in culture media at a final concentration of ~200,000 cells/mL. DAPI staining solution (Sigma-Aldrich Cat# D9542-5MG) was added to the cells at a final concentration of 0.1 ug/mL. Afterward, the cells were strained through a 35 um mesh cell strainer, directly into a 5 mL polystyrene tube (Corning Cat# 352235), and stored on ice until sorting. The FACSAria Fusion Flow

Cytometer (BD Biosciences) was used to single cell sort the population. The gates were set to filter all duplexed or multiplexed cells and the 405 nm laser was used to select out the membrane compromised population fluorescing due to DNA staining from DAPI. The cells were then individually sorted into the wells of four 96-well tissue culture plates with 200 uL of prewarmed DMEM, supplemented with 20% FBS. Once each plate was sorted, they were immediately placed in the incubator and cultured for 10-21 days, with media changed every XX days, to allow for expansion of the single cell colonies.

Once the single cell colonies reached >50% confluency, they were transferred to a 24-well plate and cultured for one week. When the cells reached >70% confluent, they were detached using Accutase and resuspended in BLANK. 40% of the cell suspensions were replated in 24-well plates and the rest of the cells were transferred to a 1.5 mL tubes and centrifuged for 5 minutes at 500 xg using a tabletop centrifuge. Following centrifugation, the supernatant was discarded, and the pelleted cells were resuspended using 10 uL of TE buffer. The resuspensions were transferred to 0.2 mL PCR strip tubes. A thermocycler was used to lyse the membranes of resuspended cells by incubating them at 95C for 10 minutes. The cells were then chilled on ice for 10 seconds. Afterward, PCR was performed to amplify different regions of the ZFP36L2 genomic region using GoTaq polymerase master mix (Promega Cat#M712) and primer oligos generated from the ApE file (Table 6). To minimize interference from secondary structures, 5% DMSO was added to all PCR reactions. PCR samples were then run on either a 1% or 1.5% agarose gel, containing SyBr Safe (Apex, Cat#A8743) gel stain solution. PCR bands of interest were excised and purified using a gel DNA extraction kit (Zymo Research, Cat#D4007) or the PCR reaction was purified using a PCR purification kit (Zymo Research, Cat#D4013).

Table 6: Primer pairs used for screening the genomic regions of ZFP36L2

Forward Primer	Forward Primer Sequence	Reverse Primer	Reverse Primer Sequence	Spanning ZFP36L2 Region of Interest	Expected size in Wildtype (bp)
screening_primer_F1	TCCAGAAACATGTCGACCAC	screening_primer_R1	GCATGTTGTTCAGGTTGAGGT	Exon-1, Intron-1, and Exon-2	593
screening_primer_F2	CTGTCCTCAGAGTCAGCTCC	screening_primer_R2	TGAACCGCCTTCCCTTCCTC	Promoter Region to the 3' UTR	3155
screening_primer_F3	GCCCTGTTTACTGAGCCTGGGC	screening_primer_R3	CACGACGAATAACGGGCGAGGG	Promoter Region	894
screening_primer_F4	TCCTCGCTTCTCTCCTTCCCCC	screening_primer_R4	TTTCGACACGTGATCCTCCGCC	5' UTR to Intron-1	532
screening_primer_F5	TGCGCGTGTATAGGTGGAGGGT	screening_primer_R5	CGCGTGGAGTTGATCTGGGAGC	Intron-1 to Exon-2	565
screening_primer_F6	ATTCCGGGACCGCTCGTTTAGC	screening_primer_R6	AACAGGAGGAGGCGGAGGGA	Exon-2	567
screening_primer_F7	TTCCCGTCGGGCCACCATCA	screening_primer_R7	TCGAACACGGGCGAGTCGGA	Exon-2	545
screening_primer_F8	TCGCCGCCCTTCAGCTTCCA	screening_primer_R8	GGTAGCTGCTGGTGCTGGGTTG	Exon-2 to 3' UTR	608

alamarBlue Cell Proliferation Assay

To measure cell proliferation, HeLa cells were cultured and harvested at 85% confluency as described above. Cells were washed once with PBS and detached using 0.05% Trypsin. Cells were then resuspended in media and stained with trypan blue to confirm cell viability was >95%. Five thousand cells were plated in triplicates, using a 96-well plate with 100 uL media. Four sets of triplicates were plated to be analyzed at four-time points (22 hr, 46 hr, 70 hr, 94 hr). Cells were incubated at 37C at 5% CO2 for their designated duration. Afterward, 11 uL of alamarBlue reagent was added to each well and incubated for 2 hours. 100 uL of each well was then transferred to a clear, flat-bottomed 96-well plate and fluorescence was measured using the Tecan plate reader. Excitation and emission wavelengths were set to 570 nm and 685 nm, respectively.

Cell Count Proliferation Assay

0.5 mL of culturing media was added to each well of a 24-well plate. 15k HeLa cells (wild type and heterozygous knockouts) were plated in triplicates, in replicate sets of 3. Every 24 hours, one replicate set had its culturing media aspirated, then was with 0.5 mL or PBS and tripsinized using 0.2 mL of 0.25% trypsin+EDTA. After addition of trypsin, cells were incubated at 37C for 5 minutes to detach from the wells. 0.2 mL of culturing media was then added to the cells. All cells were then transferred to a 1.5 mL tube and spun down at 0.3 xg for 3 minutes. The media was aspirated, and the cells were resuspended in 0.1 uL of PBS. 10 uL of the resuspended cells was mixed with 10 uL of tryphan blue stain and loaded onto a Bio-Rad cell counter slide, in duplicates. Both

duplicates had cell counts measured using the Bio-Rad cell counter. Total cell counts were determined by multiplying the percent of cells alive by the concentration of live cells, divided by 0.1 mL. The final value was then used to plot total counts for each timepoint.

Exon-Intron Splice Analysis on ZFP36L2 Knockout Data in MOLM-13 cells.

RNA-seq data from Wang et al was obtained from the gene expression omnibus using the GEO# GSE146469. All seven RNA-seq sample data (3 sets for control, 2 sets for ZFP36L2$^{(-/-)}$-1, 2 sets for ZFP36L2$^{(-/-)}$-2) was download. The human annotation file, https://ftp.ebi.ac.uk/pub/databases/gencode/Gencode_human/release_40/gencode.v40.annotation.gtf.gz, was also downloaded from gencodegenes.org. A STAR index file was then generated using the annotation file. The fasta files were then mapped to the human genome using miniconda3 tools and BAM files were generated. Mapped reads were than assigned counts using the featureCounts function. From there on, the R language was utilized to conduct exon-intron splice analysis using the BiocManager package, “eisaR”.

Citations

Bae, Sangsu, et al. “CAS-OFFinder: A Fast and Versatile Algorithm That Searches for Potential off-Target Sites of cas9 RNA-Guided Endonucleases.” *OUP Academic*, Oxford University Press, 24 Jan. 2014, https://academic.oup.com/bioinformatics/article/30/10/1473/267560.

Bertucci, F., Salas, S., Eysteries, S., Nasser, V., Finetti, P., Ginestier, C., Charafe-Jauffret, E., Loriod, B., Bachelart, L., Montfort, J., Victorero, G., Viret, F., Ollendorff, V., Fert, V., Giovaninni, M., Delpero, J. R., Nguyen, C., Viens, P., Monges, G., … Houlgatte, R. (2004). Gene expression profiling of colon cancer by DNA microarrays and correlation with histoclinical parameters. *Oncogene*, *23*(7). https://doi.org/10.1038/sj.onc.1207262Bian, X., Liang, Z., Feng, A., Salgado, E., & Shim, H. (2018). HDAC inhibitor suppresses proliferation and invasion of breast cancer cells through regulation of miR-200c targeting CRKL. *Biochemical Pharmacology*, *147*. https://doi.org/10.1016/j.bcp.2017.11.008

Cai, C., He, H. H., Chen, S., Coleman, I., Wang, H., Fang, Z., Chen, S., Nelson, P. S., Liu, X. S., Brown, M., & Balk, S. P. (2011). Androgen Receptor Gene Expression in Prostate Cancer Is Directly Suppressed by the Androgen Receptor Through Recruitment of Lysine-Specific Demethylase 1. *Cancer Cell*, *20*(4). https://doi.org/10.1016/j.ccr.2011.09.001

Che Mat, Mohd Firdaus, et al. “Silencing of ZFP36L2 Increases Sensitivity to Temozolomide through G2/M Cell Cycle Arrest and Bax Mediated Apoptosis in GBM Cells - Molecular Biology Reports.” *SpringerLink*, Springer Netherlands, 15 Feb. 2021, https://link.springer.com/article/10.1007/s11033-021-06144-z.

Chen, Min-Yu, et al. “Decitabine and Suberoylanilide Hydroxamic Acid (Saha) Inhibit Growth of Ovarian Cancer Cell Lines and Xenografts While Inducing Expression of Imprinted Tumor Suppressor Genes, Apoptosis, G2/M Arrest, and Autophagy.” *Cancer*, U.S. National Library of Medicine, 1 Oct. 2011, https://www.ncbi.nlm.nih.gov/pmc/articles/PMC3137708/#:~:text=Ovarian%20cancer%20cells%20%28Hey%20and%20SKOv3%29%20were%20treated,PEG3%2C%20two%20growth%20inhibitory%20imprinted%20tumor%20suppressor%20genes.

Doench JG;Fusi N;Sullender M;Hegde M;Vaimberg EW;Donovan KF;Smith I;Tothova Z;Wilen C;Orchard R;Virgin HW;Listgarten J;Root DE; “Optimized Sgrna Design to Maximize Activity and Minimize off-Target Effects of CRISPR-Cas9.” *Nature Biotechnology*, U.S. National Library of Medicine, https://pubmed.ncbi.nlm.nih.gov/26780180/.

Draizen EJ;Shaytan AK;Mariño-Ramírez L;Talbert PB;Landsman D;Panchenko AR; “HistoneDB 2.0: A Histone Database with Variants--an Integrated Resource to Explore Histones and Their Variants.” *Database : the Journal of Biological Databases and Curation*, U.S. National Library of Medicine, https://pubmed.ncbi.nlm.nih.gov/26989147/.

Dumdie, J. N., Cho, K., Ramaiah, M., Skarbrevik, D., Mora-Castilla, S., Stumpo, D. J., Lykke-Andersen, J., Laurent, L. C., Blackshear, P. J., Wilkinson, M. F., & Cook-Andersen, H. (2018). Chromatin Modification and Global Transcriptional Silencing in the Oocyte Mediated by the mRNA Decay Activator ZFP36L2. *Developmental Cell*, *44*(3). https://doi.org/10.1016/j.devcel.2018.01.006

Dupré A;Berhane S;Chan AWH;Rivoire M;Chong CCN;Lai PBS;Cucchetti A;Poston GJ;Malik HZ;Johnson PJ; "Multicentre Validation of a Clinical Prognostic Score Integrating the Systemic Inflammatory Response to the Host for Patients Treated with Curative-Intent for Colorectal Liver Metastases: The Liverpool Score." *European Journal of Surgical Oncology : the Journal of the European Society of Surgical Oncology and the British Association of Surgical Oncology*, U.S. National Library of Medicine, https://pubmed.ncbi.nlm.nih.gov/30827803/.

Elvir, Lindsay, et al. "Epigenetic Regulation of Motivated Behaviors by Histone Deacetylase Inhibitors." *Neuroscience and Biobehavioral Reviews*, U.S. National Library of Medicine, Oct. 2019, https://www.ncbi.nlm.nih.gov/pmc/articles/PMC5889966/.

Fallmann, Jörg, et al. "Aresite2: An Enhanced Database for the Comprehensive Investigation of Au/Gu/U-Rich Elements." *OUP Academic*, Oxford University Press, 23 Nov. 2015, https://academic.oup.com/nar/article/44/D1/D90/2503047?login=false.

Hou X;Li Q;Yang L;Yang Z;He J;Li Q;Li D; "KDM1A And KDM3A Promote Tumor Growth by Upregulating Cell Cycle-Associated Genes in Pancreatic Cancer." *Experimental Biology and Medicine (Maywood, N.J.)*, U.S. National Library of Medicine, https://pubmed.ncbi.nlm.nih.gov/34171978/.

Gaidatzis, Dimos, et al. "Analysis of Intronic and Exonic Reads in RNA-Seq Data Characterizes Transcriptional and Post-Transcriptional Regulation." *Nature News*, Nature Publishing Group, 22 June 2015, https://www.nature.com/articles/nbt.3269.

Herzog, Veronika A, et al. "Thiol-Linked Alkylation of RNA to Assess Expression Dynamics." *Nature News*, Nature Publishing Group, 25 Sept. 2017, https://www.nature.com/articles/nmeth.4435.

Hsiang, M. W., & Cole, R. D. (1977). Structure of histone H1-DNA complex: Effect of histone H1 on DNA condensation. *Proceedings of the National Academy of Sciences of the United States of America*, *74*(11). https://doi.org/10.1073/pnas.74.11.4852

Hsu, Patrick D, et al. "DNA Targeting Specificity of RNA-Guided cas9 Nucleases." *Nature News*, Nature Publishing Group, 21 July 2013, https://www.nature.com/articles/nbt.2647.

Ishimura, A., Terashima, M., Kimura, H., Akagi, K., Suzuki, Y., Sugano, S., & Suzuki, T. (2009). Jmjd2c histone demethylase enhances the expression of Mdm2 oncogene. *Biochemical and Biophysical Research Communications*, *389*(2). https://doi.org/10.1016/j.bbrc.2009.08.155

Kahl, P., Gullotti, L., Heukamp, L. C., Wolf, S., Friedrichs, N., Vorreuther, R., Solleder, G., Bastian, P. J., Ellinger, J., Metzger, E., Schüle, R., & Buettner, R. (2006). Androgen receptor coactivators lysine-specific histone demethylase 1 and four and a half LIM domain protein 2 predict risk of prostate cancer recurrence. *Cancer Research*, *66*(23). https://doi.org/10.1158/0008-5472.CAN-06-1570

Kim, K. C., Geng, L., & Huang, S. (2003). Inactivation of a Histone Methyltransferase by Mutations in Human Cancers. *Cancer Research*, *63*(22).

Kim, S., Bolatkan, A., Kaneko, S., Ikawa, N., Asada, K., Komatsu, M., Hayami, S., Ojima, H., Abe, N., Yamaue, H., & Hamamoto, R. (2019). Deregulation of the histone lysine-specific demethylase 1 is involved in human hepatocellular carcinoma. *Biomolecules*, *9*(12). https://doi.org/10.3390/biom9120810

Klose, R. J., Yamane, K., Bae, Y., Zhang, D., Erdjument-Bromage, H., Tempst, P., Wong, J., & Zhang, Y. (2006). The transcriptional repressor JHDM3A demethylates trimethyl histone H3 lysine 9 and lysine 36. *Nature*, *442*(7100). https://doi.org/10.1038/nature04853

Kogure, M., Takawa, M., Cho, H. S., Toyokawa, G., Hayashi, K., Tsunoda, T., Kobayashi, T., Daigo, Y., Sugiyama, M., Atomi, Y., Nakamura, Y., & Hamamoto, R. (2013). Deregulation of the histone demethylase JMJD2A is involved in human carcinogenesis through regulation of the G1/S transition. *Cancer Letters*, *336*(1). https://doi.org/10.1016/j.canlet.2013.04.009

Kouzarides, T. (2007). Chromatin Modifications and Their Function. In *Cell* (Vol. 128, Issue 4). https://doi.org/10.1016/j.cell.2007.02.005

Liu, J., Lu, W., Liu, S., Wang, Y., Li, S., Xu, Y., Xing, H., Tang, K., Tian, Z., Rao, Q., Wang, M., & Wang, J. (2018). ZFP36L2, a novel AML1 target gene, induces AML cells apoptosis and inhibits cell proliferation. *Leukemia Research*, *68*. https://doi.org/10.1016/j.leukres.2018.02.017

Lykke-Andersen, J., & Wagner, E. (2005). Recruitment and activation of mRNA decay enzymes by two ARE-mediated decay activation domains in the proteins TTP and BRF-1. *Genes and Development*, *19*(3). https://doi.org/10.1101/gad.1282305

Mohammad, H. P., Barbash, O., & Creasy, C. L. (2019). Targeting epigenetic modifications in cancer therapy: erasing the roadmap to cancer. In *Nature Medicine* (Vol. 25, Issue 3). https://doi.org/10.1038/s41591-019-0376-8

Mukherjee, N., Jacobs, N. C., Hafner, M., Kennington, E. A., Nusbaum, J. D., Tuschl, T., Blackshear, P. J., & Ohler, U. (2014). Global target mRNA specification and regulation by the RNA-binding protein ZFP36. *Genome Biology*, *15*(1). https://doi.org/10.1186/gb-2014-15-1-r12

Perry, R. P., & Kelley, D. E. (1970). Inhibition of RNA synthesis by actinomycin D: Characteristic dose-response of different RNA species. *Journal of Cellular Physiology*, *76*(2). https://doi.org/10.1002/jcp.1040760202

Sakamoto, S., Potla, R., & Larner, A. C. (2004). Histone deacetylase activity is required to recruit RNA polymerase II to the promoters of selected interferon-stimulated early response genes. *Journal of Biological Chemistry*, *279*(39). https://doi.org/10.1074/jbc.M406400200

Skov, V., Thomassen, M., Kjær, L., Larsen, T. S., Kruse, T. A., & Hasselbalch, H. (2019). Highly Deregulated Fibulins in Patients with Philadelphia-Negative Chronic Myeloproliferative Neoplasms. *Blood*, *134*(Supplement_1). https://doi.org/10.1182/blood-2019-130560

Said, Thenaa K, et al. "Mechanisms of Suberoylanilide Hydroxamic Acid Inhibition of Mammary Cell Growth - Breast Cancer Research." *BioMed Central*, BioMed Central, 22 Dec. 2000, https://breast-cancer-research.biomedcentral.com/articles/10.1186/bcr284#:~:text=The%20mechanism%20of%20suberoylanilide%20hydroxamic%20acid%20in%20cell,synthesis%20in%20mammary%20epithelial%20cell%20lines.%20Synopsis%20Background.

Spasic, Milan, et al. "Genome-Wide Assessment of Au-Rich Elements by the AREScore Algorithm." *PLOS Genetics*, Public Library of Science, http://www.plosgenetics.org/article/info%3Adoi%2F10.1371%2Fjournal.pgen.1002433.

Suk, F. M., Chang, C. C., Lin, R. J., Lin, S. Y., Liu, S. C., Jau, C. F., & Liang, Y. C. (2018). ZFP36L1 and ZFP36L2 inhibit cell proliferation in a cyclin D-dependent and p53-independent manner. *Scientific Reports*, *8*(1), 1–13. https://doi.org/10.1038/s41598-018-21160-z

Suraweera, A., O'Byrne, K. J., & Richard, D. J. (2018). Combination therapy with histone deacetylase inhibitors (HDACi) for the treatment of cancer: Achieving the full therapeutic potential of HDACi. In *Frontiers in Oncology* (Vol. 8, Issue MAR). https://doi.org/10.3389/fonc.2018.00092

Tamaru, Hisashi. "Confining Euchromatin/Heterochromatin Territory: Jumonji Crosses the Line." *Genes & Development*, Cold Spring Harbor Lab, 1 Jan. 1970, http://genesdev.cshlp.org/content/24/14/1465/F2.expansion.html.

W;, Straining R;Eighmy. "Tazemetostat: EZH2 Inhibitor." *Journal of the Advanced Practitioner in Oncology*, U.S. National Library of Medicine, https://pubmed.ncbi.nlm.nih.gov/35369397/.

Wang, Eric, et al. "Surface Antigen-Guided CRISPR Screens Identify Regulators of Myeloid Leukemia Differentiation." *Cell Stem Cell*, Cell Press, 14 Jan. 2021, https://www.sciencedirect.com/science/article/pii/S1934590920305890#sec4.

Wang, Y., Zhu, L., Guo, M., Sun, G., Zhou, K., Pang, W., Cao, D., Tang, X., & Meng, X. (2021). Histone methyltransferase WHSC1 inhibits colorectal cancer cell apoptosis via targeting anti-apoptotic BCL2. *Cell Death Discovery*, *7*(1). https://doi.org/10.1038/s41420-021-00402-6